Specific binding of urinary-type plasminogen activator (u-PA) to vitronectin and its role in mediating u-PA-dependent adhesion of U937 cells

Tammy L. MOSER,* Jan J. ENGHILD,* Salvatore V. PIZZO* and M. Sharon STACK†‡

*Department of Pathology, Duke University Medical Center, Durham, NC 27710
and †Department of Obstetrics and Gynecology, Northwestern University, Chicago, IL 60611, U.S.A.

The present paper described interactions of urinary-type plasminogen activator (u-PA) with isolated protein components of the extracellular matrix (ECM) using kinetic and ligand-blotting analyses, as well as adhesion studies with uPA-saturated U937 monocytic cells. Kinetic analyses showed that fibronectin and laminin were moderately effective at decreasing activation of plasminogen by u-PA (3–4-fold decrease in $k_{cat.}/K_m$), while activation was stimulated slightly by collagen types I and IV (2–4-fold increase in $k_{cat.}/K_m$). Ligand-blotting experiments using intact immobilized ECM proteins demonstrated that u-PA binds predominantly to vitronectin. This was supported by ELISA studies, which showed concentration dependent, saturable, reversible binding of u-PA to vitronectin ($K_{d,app.}$ of 97 nM). Limited proteolysis of vitronectin followed by ligand-blotting analysis demonstrated u-PA binding to a specific vitronectin fragment (M_r 49000), and binding was shown to occur through the N-terminal fragment of u-PA. N-terminal sequence analysis indicated that this binding fragment of vitronectin originates with Thr-122 and comprises the hemopexin domain, including the heparin-binding region of the vitronectin molecule. Plasminogen activator inhibitor type I did not compete with u-PA for binding to vitronectin, suggesting both molecules may co-localize on vitronectin. In contrast, binding of u-PA to vitronectin was significantly inhibited by plasminogen, suggesting these molecules share a common binding site on vitronectin. In addition to *in vitro* studies, experiments were performed to assess the contribution of direct binding of u-PA to vitronectin on the adhesive behaviour of U937 cells. Binding of u-PA-saturated U937 cells to vitronectin was inhibited 66% by excess vitronectin, suggesting that direct binding of u-PA to vitronectin is the mechanism by which u-PA-dependent adhesion of U937 cells to vitronectin is mediated.

INTRODUCTION

Urinary-type plasminogen activator (u-PA) and tissue-type plasminogen activator (t-PA) are serine proteinases which function to convert the zymogen plasminogen (Pg) into the active proteinase plasmin. Whereas u-PA-catalysed Pg activation is associated with the initiation of pericellular proteolysis, t-PA is associated predominantly with fibrinolysis [1–3]. Plasmin has been implicated in numerous physiological and pathological processes involving ECM remodelling, including inflammation, wound healing and tumour migration [4–6]. Current models for regulation of plasmin formation suggest that Pg activation is a surface-associated process whereby binding of the zymogen, the activator, or both to a surface can modulate the kinetics of zymogen activation as well as the association of active enzyme with specific proteinase inhibitors. In fibrinolysis, both Pg and t-PA bind specifically to the fibrin clot surface, resulting in enhanced efficiency of Pg activation [7,8]. In addition to fibrin, numerous studies have demonstrated that intact ECM as well as individual matrix-associated macromolecules such as collagen, fibronectin, laminin and vitronectin may regulate t-PA catalysed Pg activation [9–15].

Recent studies have demonstrated that u-PA can also interact specifically with ECM-associated macromolecules including heparin, thrombospondin, laminin and nidogen, suggesting that direct matrix interactions may also regulate u-PA activity [16–18]. In addition, the activity of u-PA is localized by high-affinity binding to a specific cell-surface receptor (designated u-PA receptor or uPAR) found on a variety of normal and neoplastic cells [19,20]. Many cell types also contain high-capacity, low-affinity binding sites for Pg [21]. Several studies have demonstrated that co-localization of Pg and u-PA results in the generation of plasmin on the cell surface [22,23]. Although u-PA bound to uPAR remains susceptible to inhibition by plasminogen activator inhibitor (PAI-1), surface-associated plasmin is not efficiently inactivated by the plasmin inhibitor α_2-antiplasmin, thereby providing a mechanism for generation of enhanced plasmin-mediated pericellular proteolysis [24,21]. Furthermore, uPAR occupancy has been linked to increased adherence of monocytic cells to matrix-associated vitronectin, suggesting a direct role of u-PA in regulation of cell–matrix adhesion [25,26].

The present study investigates binding and kinetic interactions of u-PA with a variety of ECM-associated proteins. We report specific binding of u-PA to the matrix-associated glycoprotein vitronectin and have localized the binding region to an M_r-49000 fragment comprising the hemopexin domain, including the heparin-binding region of vitronectin. The amino-(N-) terminal fragment (ATF; amino acids 1–135, containing both the growth factor and kringle domains [27]) of u-PA mediates binding to vitronectin, whereas no binding to low-M_r u-PA (amino acids

Abbreviations used: u-PA, urinary-type plasminogen activator; t-PA, tissue-type plasminogen activator; ECM, extracellular matrix; Pg, plasminogen; PAI-1, plasminogen activator inhibitor; uPAR, urinary-type plasminogen activator receptor; ATF, amino (N-)terminal fragment; VLK-pNA, D-Val-Leu-Lys *p*-nitroanilide; DCI, dichloroisocoumarin; BCIP, 5-bromo-chloroindol-3-yl phosphate; NBT, Nitro Blue Tetrazolium; PMA, phorbol 12-myristate 13-acetate; PVDF, poly(vinylidene difluoride); IPR-pNA, D-Ile-Pro-Arg *p*-nitroanilide; DFP, di-isopropyl fluorophosphate; MEME, Eagle's minimal essential medium.

‡ To whom correspondence should be addressed.

136–411 containing the catalytic domain [27]) is observed. These studies provide further evidence for direct interaction of u-PA with ECM macromolecules and suggest a mechanism whereby uPAR occupancy may regulate cell adhesion to vitronectin.

EXPERIMENTAL

Materials

BSA, anti-(goat IgG)–alkaline phosphatase conjugate, anti-(rabbit IgG)–alkaline phosphatase conjugate, D-Val-Leu-Lys *p*-nitroanilide (VLK-pNA or S2251), dichloroisocoumarin (DCI), fibronectin from human plasma, murine Engelbreth–Holm–Swarm-sarcoma laminin, human collagen types I and IV, 5-bromo-4-chloroindol-3-yl phosphate (BCIP), Nitro Blue Tetrazolium (NBT) tablets, cell-culture reagents, phorbol 12-myristate 13-acetate (PMA) and endoproteinase Glu-C from *Staphylococcus aureus* strain V8 (endoproteinase V8) were purchased from Sigma Chemical Co., St. Louis, MO, U.S.A. Poly(vinylene difluoride) membranes (PVDF) were purchased from Millipore, Bedford, MA, U.S.A. Rabbit anti-(human vitronectin) affinity purified IgG antibody was purchased from Telios, Bedford, MA, U.S.A. D-Ile-Pro-Arg *p*-nitroanilide (IPR-pNA or S2288) was purchased from Helena Laboratories, Beaumont, TX, U.S.A. High-M_r and low-M_r human urokinase (containing only the serine-proteinase domain) were purchased from Calbiochem, San Diego, CA, U.S.A. and protein concentrations were supplied by the manufacturer. High-M_r urokinase was used for all experiments unless otherwise specified. Urokinase was coupled to CNBr-activated Sepharose 4B by the method of Cuatrecasas et al. [28]. Di-isopropyl fluorophosphate (DFP) inactivated u-PA was prepared as described by Behrendt et al. [29]. ATF, comprising residues 3–35 and encompassing the uPAR-binding domain, was generously given by Dr. Jack Henkin, Abbott Laboratories, Abbott Park, IL, U.S.A. PAI-1 was purchased from American Diagnostica, Greenwich, CT, U.S.A. or was generously given by Dr. David Ginsberg, University of Michigan Medical Center, Ann Arbor, MI, U.S.A. All other chemicals were of reagent-grade quality.

Proteins

Pg was purified from human plasma by affinity chromatography on L-lysine–Sepharose [30]. Pg isoforms 1 and 2 were separated by affinity chromatography on concanavalin A–Sepharose [31]. Affinity chromatography purified form 2 was utilized for all experiments. On the basis of kinetic and electrophoretic analysis, all Pg preparations were shown to be plasmin-free. Plasmin was generated by incubating 100 μg of Pg with 100 μl of u-PA–Sepharose in 10 mM Hepes, pH 7.4, for 1 h at 25 °C, followed by centrifugation to remove the resin. Protein concentrations were determined spectrophotometrically at 280 nm using an $A^{1\,cm}_{1\%}$ value of 16.8 and M_r values of 92 and 81 kDa for Pg and plasmin respectively [2]. Native vitronectin was purified using a modification of the procedure described by Dahlback and Podack [32], which consists of an additional FPLC purification step using Mono Q HR5/5 Sepharose (Pharmacia, Piscataway, NJ, U.S.A.). Pure vitronectin was eluted using a linear gradient from 50 mM Tris/HCl, pH 7.4 to 50 mM Tris/HCl, pH 7.4/1 M NaCl. Radioiodination of u-PA and vitronectin was performed using Enzymobeads (Bio-Rad) according to manufacturer's specifications. Radioactivity was measured using an LKB 1272 γ-radiation counter. Radioactive blots were analysed by using a Molecular Dynamics PhosphorImager (Sunnyvale, CA, U.S.A.).

Kinetic analysis of Pg activation

Coupled assays were used to evaluate the initial rate of Pg activation by u-PA by monitoring the amidolytic activity of generated plasmin [33]. Pg (0–2.0 μM) was incubated at 37 °C for 15 min in 20 mM Hepes, pH 7.4, with the plasmin substrate VLK-pNA (0.3 mM final concn.) and 0.5 μM of the indicated protein. Activation of Pg was initiated by addition of 1.5 pM u-PA and the plasmin hydrolysis of VLK-pNA was monitored continuously at 405 nm. Initial velocities (v_i) were calculated from the slope (b) of plots of A_{405} versus time^2 by using the equation:

$$v_i = b(1 + K_m/S_o)/\epsilon k_e \quad [33]$$

where K_m is the apparent Michaelis constant of VLK-pNA hydrolysis by plasmin (3×10^{-4} M), k_e is the empirically determined catalytic rate constant for plasmin hydrolysis of VLK-pNA (3.2×10^4 M·min^{-1}·mol of plasmin^{-1}) and ϵ is the molar absorption coefficient of *p*-nitroanilide at 405 nm (8800 M^{-1}·cm^{-1}; Erlanger et al. [34]). Reaction mixtures containing collagen were also performed with buffers containing 0.25 M glucose to prevent collagen fibril formation [35]. Activation reactions were also performed as described above on protein-coated microtitre plates. Plates were coated by passive adsorption using 5.0 μg/ml fibronectin, vitronectin, collagen type I, collagen type IV and 10.0 μg/ml laminin as previously described by [13]. All experiments were repeated a minimum of 10 times using two different preparations of Pg. Data were analysed by the method of Lineweaver and Burk [36] to evaluate kinetic constants.

Ligand-blot assay

In studies examining the binding of u-PA to immobilized intact fibronectin, laminin, vitronectin, collagen type I, and collagen type IV, 10 μg of protein were electrophoresed on SDS/7.5% polyacrylamide gels [37] and electroblotted on to PVDF membranes [38]. After electroblotting, one membrane was stained with Coomassie Blue for protein identification. Before ligand-binding studies, blots were incubated in 10 mM Tris/HCl/0.15 M NaCl/0.05% Nonidet P40/1% BSA, pH 7.5 (TSN buffer), for 1 h at room temperature to block non-specific sites. After blocking with TSN buffer, blots were incubated overnight with ^{125}I-labelled u-PA (1×10^6 c.p.m.) in 5 ml of TSN buffer. Blots were washed four times for 5 min each in 10 mM Tris/HCl/0.15 M NaCl/0.05% Tween 80/1% BSA, pH 7.5 (TS/Tween buffer), and allowed to dry before viewing on the PhosphorImager. All blot-binding studies were performed a minimum of five times.

ELISA

ELISA binding studies were performed with vitronectin passively adsorbed on medium-binding polystyrene(a) 96-well flat-bottomed culture plates (Costar, Cambridge, MA, U.S.A.) as previously described by Moser et al. [14]. Briefly, plates were coated with 200 μl of vitronectin in 0.1 M Na_2CO_3 (pH 9.6)/0.02% NaN_3 and incubated overnight at 5 °C. The amount of vitronectin coated using this procedure was determined using ^{125}I-labelled vitronectin (1.3×10^6 c.p.m./μg). Under these conditions, the amount of vitronectin adsorbed was 164 ng/well (2.5 pmol/well). Before ELISA, non-specific sites were blocked by incubating with TS/Tween containing 3% BSA for 1 h at

room temperature. For binding studies, increasing amounts of u-PA (0–450 nM) were added in a 200 μl final volume of TS/Tween. Plates were washed and incubated with goat anti-(human urokinase IgG) antibody (1:5000) for 1 h at room temperature. Then plates were washed and incubated with anti-(goat IgG) antibody–alkaline phosphate conjugate (1:2000) for 30 min at room temperature. Plates were again washed and 200 μl of alkaline phosphatase substrate (1 mg of *p*-nitrophenyl phosphate substrate/ml in 0.1 M glycine buffer (pH 10.4)/1 mM $MgCl_2$/1 mM $ZnCl_2$) were added to the plate and adsorbance was monitored at 405 nm using a Molecular Devices Thermomax kinetic plate reader. All experiments were repeated a minimum of eight times. Apparent binding affinities ($K_{d,app.}$) were calculated by non-linear regression analysis of the data using the standard binding isotherm equation from the DNRPEasy program (version 3.55 by R. G. Duggleby and D. R. Leonard, Biochemistry Department, University of Queensland, St. Lucia, Qld. 4072, Australia) on an IBM PS/Value Point 433 DX computer.

Competition ELISA binding studies were performed to determine the ability of solution-phase proteins to compete for u-PA binding to vitronectin-coated plates. Increasing amounts of Pg (0–200 nM), PAI-1 (0–500 nM), or vitronectin (0–1000 nM) were added in the presence of DFP-u-PA (100 nM) to plates coated with vitronectin. u-PA binding was analysed as described above.

Binding of u-PA to vitronectin and vitronectin fragments

In studies examining the binding of u-PA to vitronectin, limited proteolysis of vitronectin was carried out using endoproteinase V8 as previously described [14]. The reaction was inhibited by the addition of 0.1 mM DCI, and samples were boiled immediately, electrophoresed on SDS/5–15%-gradient PAGE gels, and transferred to PVDF. The M_r values for the vitronectin fragments were determined by comparison with the migration of standard proteins (Bio-Rad, Hercules, CA, U.S.A.) on SDS/5–15%-PAGE gels. After the transfer, one membrane was stained with Coomassie Blue for protein identification. The other membrane was blocked with TSN buffer and incubated overnight with either ^{125}I-labelled u-PA or ^{125}I-labelled ATF (1×10^6 c.p.m.) in 10 ml of TSN buffer. Blots were washed as described above, air-dried and analysed using a PhosphorImager. Binding studies with u-PA were repeated a minimum of eight times, whereas studies using ATF were performed in triplicate. The amino acid sequences of specific vitronectin polypeptides were determined using an Applied Biosystems 477A pulse liquid-phase sequencer with 'on-line' 120A phenylthiohydantoin analysis. Vitronectin polypeptides were separated by SDS/PAGE, transferred to PVDF, and stained with Coomassie Blue, and the bands of interest were excised, placed on Porton sample support discs, and sequenced.

Vitronectin binding to domains of u-PA

In studies examining the binding of vitronectin to u-PA domains, 3.7 μg of ATF or 3.2 μg low-M_r u-PA were electrophoresed on SDS/5–15%-PAGE gels and electroblotted as described above. After electroblotting, one membrane was stained with Coomassie Blue for protein identification and the other membrane was incubated overnight with ^{125}I-vitronectin (1×10^6 c.p.m.) in 5 ml of TSN buffer. Blots were washed and analysed as described above. Binding studies were performed in triplicate.

u-PA-mediated U937 adhesion to vitronectin

The U937 monocytoid leukaemia cell line was generously given by Dr. Mario Gonzalez-Gronow, Duke University Medical Center, Durham, NC, U.S.A., and grown in Eagle's minimal essential medium (MEME) containing 5% (v/v) fetal-calf serum, non-essential amino acids, L-glutamine, vitamins and penicillin–streptomycin. Before each experiment, cells were stimulated for 24 h with 16 nM PMA and washed in PBS without Mg^{2+} and Ca^{2+} as described by Behrendt [39]. uPAR occupancy on U937 cells was saturated by incubation with 10 nM DFP-u-PA in MEME containing 1 mg/ml BSA at 4 °C for 90 min [39]. Adhesion of u-PA-saturated U937 cells to immobilized vitronectin was performed as described in Waltz and Chapman [26]. After incubation, bound cells were removed by trypsin treatment and counted in a haemocytometer. The ability of soluble vitronectin to inhibit binding to immobilized vitronectin was determined by incubating u-PA-saturated U937 cells with 100 nM vitronectin prior to addition to vitronectin-coated wells. Adhesion of u-PA-saturated U937 cells was carried out as described above.

RESULTS

Effect of ECM proteins on u-PA activity

In order to determine the effect of ECM proteins on regulation of u-PA activity, activation of Pg by u-PA in the presence of solution-phase ECM-associated proteins was studied. The kinetic parameters of Pg activation by u-PA in the presence of soluble ECM proteins were analysed using Lineweaver–Burk plots. As summarized in Table 1, modest effects of the ECM proteins on the activation were observed. A slight increase in catalytic efficiency ($k_{cat.}/K_m$) of Pg activation was observed in the presence of collagen types I and IV and vitronectin, and a decrease in efficiency was seen in the presence of fibronectin and laminin. The direct amidolytic activity of u-PA was also assayed in the presence of ECM protein components using IPR-pNA. The velocity of IPR-pNA hydrolysis ranged from 9.4×10^{11} to 11.5×10^{11} mol of pNA released/min, indicating no significant difference in u-PA amidolytic activity in the presence of ECM proteins relative to the BSA control (results not shown).

Binding of u-PA to intact ECM-associated proteins

Ligand-blotting assays were initially utilized to identify binding interactions between soluble u-PA and immobilized ECM proteins. Intact fibronectin, laminin, vitronectin, collagen type I

Table 1 Kinetic parameters of Pg activation by u-PA in the presence of ECM-associated proteins

Kinetic parameters were determined after incubation of the indicated ECM protein (0.5 μM) with Pg (0–2.0 μM) at 37 °C for 15 min, followed by the addition of 1.5 pM u-PA and 0.3 mM VLK-pNA. Plasmin (Pm) hydrolysis of VLK-pNA was monitored at 405 nm.

ECM protein	K_m (μM)	$V_{max.}$ (pmol of Pm/min)	$k_{cat.}$ (s^{-1})	$k_{cat.}/K_m$ ($\mu M^{-1} \cdot s^{-1}$)
No protein	1.11	18.1	1167	1051
Collagen I	0.31	16.7	1071	3455
Collagen IV	0.44	14.3	917	2084
Fibronectin	12.16	50.0	3205	264
Laminin	2.86	16.7	1071	375
Vitronectin	0.60	17.5	1122	1870

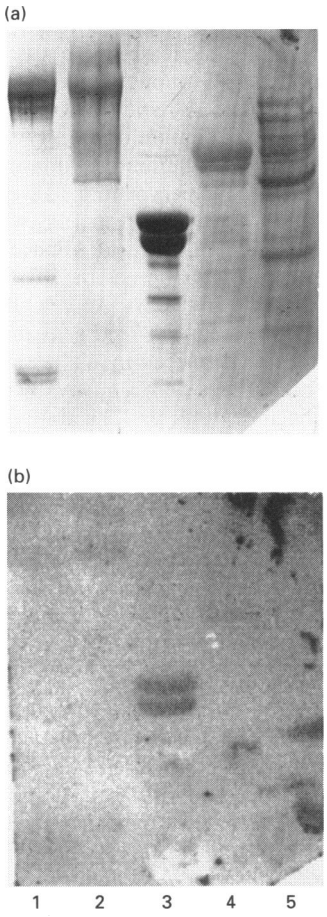

Figure 1 Binding of ^{125}I-u-PA to intact ECM proteins

Intact ECM proteins (10 μg) were electrophoresed under reducing conditions on SDS/7.5% PAGE and transferred to PVDF as described in the Experimental section. (**a**) PVDF membrane stained with Coomassie Blue; (**b**) PVDF membrane incubated with ^{125}I-u-PA. lane 1, fibronectin; lane 2, laminin; lane 3, vitronectin; lane 4, collagen type I; lane 5, collagen type IV.

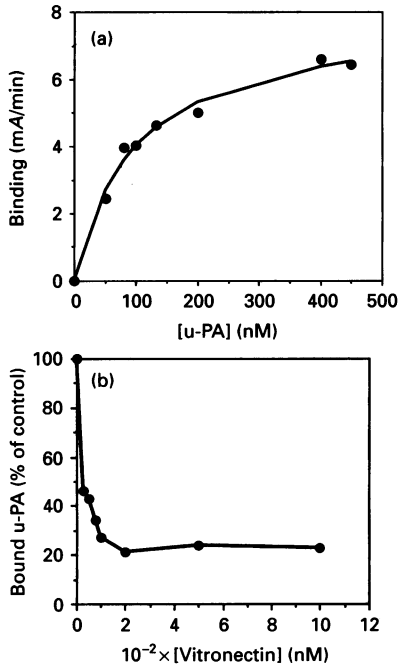

Figure 2 ELISA of u-PA binding to immobilized vitronectin

(**a**) u-PA was added in increasing concentrations to 96-well microtitre plates coated with vitronectin. Binding was analysed by ELISA as described in the Experimental section. The $K_{d,app.}$ calculated from the binding data was 97 nM. (**b**) Vitronectin (0–1000 nM) was added in increasing concentrations in the presence of 100 nM DFP–u-PA to 96-well microtitre plates coated with vitronectin. Binding of u-PA was analysed by ELISA as described in the Experimental section.

and collagen type IV were electrophoresed, blotted on to PVDF, and incubated overnight with ^{125}I-u-PA. ^{125}I-u-PA bound significantly to immobilized vitronectin (Figure 1, lane 3), with slight binding to collagen type I also observed (Figure 1, lane 4). Similar results were observed under non-reducing conditions, although the mobility of the proteins was altered slightly in the absence of reducing agent (results not shown).

Because ligand-blotting experiments indicated significant binding of u-PA to vitronectin, an ELISA was developed to examine the interaction between soluble u-PA and immobilized vitronectin. Incubation of u-PA with vitronectin passively adsorbed to microtitre wells led to concentration-dependent, saturable binding of u-PA (Figure 2a). The apparent dissociation constant ($K_{d,app.}$) calculated from the binding data was 97 nM. Binding was reversible in the presence of solution-phase vitronectin, with 80% inhibition observed with a 2-fold excess of soluble vitronectin (Figure 2b).

Binding of u-PA to vitronectin and vitronectin fragments

Because ligand-blotting and ELISA studies indicated a specific interaction between u-PA and vitronectin, additional ligand blotting assays were utilized to localize binding to a specific region of vitronectin. Vitronectin was subjected to limited proteolysis with endoproteinase V8, electrophoresed, blotted on to PVDF, and incubated with ^{125}I-u-PA. Binding of ^{125}I-u-PA to both intact and endoproteinase-V8-degraded vitronectin was observed (Figure 3b). Although at least eight distinct vitronectin fragments were generated by limited proteolysis, u-PA interacts predominately with only two of these fragments, most notably those polypeptides that migrate at an M_r of 49000 and 39000. Similar results were obtained using non-reduced vitronectin, although the mobility of the fragments was altered slightly in the absence of reducing agent (results not shown). No non-specific binding to endoproteinase V8 and M_r standards was observed. In order to determine which portion of the u-PA molecule was responsible for binding to vitronectin, ligand-blotting experiments were performed with individual u-PA domains. ATF, containing the growth factor and kringle domains, and low-M_r u-PA, comprised of the proteinase domain, were electrophoresed on a 5–15% gradient gel, blotted on to PVDF, and incubated with ^{125}I-vitronectin. Binding of vitronectin to only the ATF domain of u-PA was noted (Figure 4a). To verify the observation that ATF was responsible for the binding to the 39 and 49 kDa fragments observed in Figure 3, endoproteinase-V8-digested vitronectin was incubated with ^{125}I-ATF as previously described. As observed with intact u-PA, ATF also bound predominantly to 39 and 49 kDa fragments, as well as to intact vitronectin (Figure 4c).

To identify further which region of the vitronectin molecule was represented by the M_r-49000 fragment, amino-acid-sequence analysis was performed. The N-terminal sequence analysis indi-

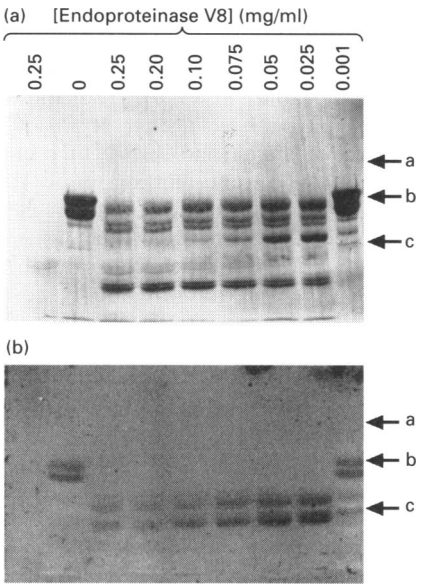

Figure 3 Binding of ^{125}I-u-PA to vitronectin and vitronectin fragments

Vitronectin (10 μg/lane) was subjected to limited proteolysis with various concentrations (mg/ml) of endoproteinase V8 as indicated for 15 min, electrophoresed under reducing conditions on SDS/5–15%-gradient-PAGE gels and transferred to PVDF as described in the Experimental section. (**a**) PVDF membrane stained with Coomassie Blue; (**b**) PVDF membrane incubated with ^{125}I-u-PA. M_r markers: a, β-galactosidase (116000); b, BSA (66,000); c, ovalbumin (45000).

cated a sequence of Thr-Leu-His-Pro-Gly-Arg-Pro-Gln-Pro-Pro. Comparison with the known sequence of vitronectin indicated that the M_r-49000 fragment started at Thr-122 and comprised the hemopexin-like domain of vitronectin containing the heparin-binding region [40,41]. Quantities of the M_r-39000 fragment were not sufficient for sequence analysis.

To ensure that the interaction between u-PA and vitronectin did not reflect an artefact of adsorption of vitronectin to a surface, binding of u-PA to intact vitronectin was also analysed in solution. Vitronectin (10 μg) was incubated with 0.3 ml of u-PA-Sepharose for 4 h at 25 °C. The reaction mixture was poured into a column, washed with 10 column volumes of 50 mM Tris/HCl, pH 7.5, and eluted with 10 column volumes of 100 mM glycine, pH 2.5. Wash and eluate fractions were freeze-dried, then analysed by electrophoresis on 5–15% gradient gels. Results from this experiment indicated that intact vitronectin bound to the u-PA–Sepharose column, demonstrating that the interaction between u-PA and vitronectin was not an artefact of immobilization or partial denaturation of vitronectin (results not shown).

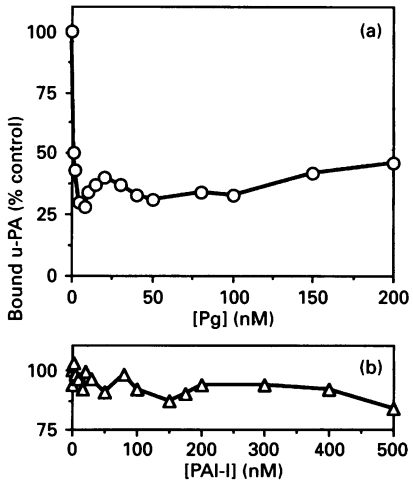

Figure 5 Competition ELISA of u-PA binding to vitronectin in the presence of Pg or PAI-1

DFP-u-PA (100 nM) was added together with increasing concentrations of Pg (0–200 nM) or PAI-1 (0–500 nM) to 96-well microtitre plates coated with vitronectin. Binding was analysed by ELISA as described in the Experimental section. (**a**) Percentage of u-PA bound in the presence of Pg; (**b**) Percentage of u-PA bound in the presence of PAI-1.

ELISA of u-PA binding to vitronectin in the presence of excess Pg or PAI-1

Because previous investigators have demonstrated binding of both Pg and PAI-1 to vitronectin, the ability of Pg and PAI-1 to

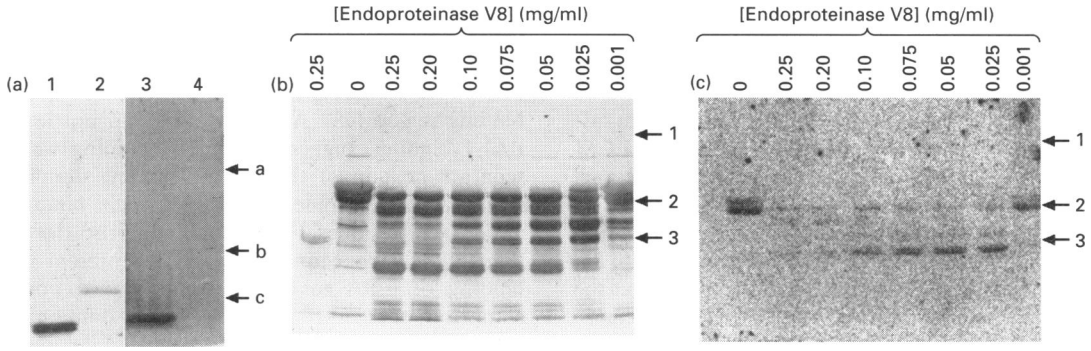

Figure 4 Identification of u-PA domains involved in vitronectin binding

(**a**) Binding of vitronectin to u-PA domain fragments. u-PA domain fragments were electrophoresed on SDS/5–15%-gradient-PAGE gels and transferred to PVDF as described in the Experimental section. Lanes 1 and 3 contained ATF (3.7 μg); lanes 2 and 4 contained low-M_r u-PA (3.2 μg). Lanes 1 and 2, PVDF membrane stained with Coomassie Blue. Staining differences reflect differential reaction of proteins with Coomassie Blue rather than large differences in protein loading. Lanes 3 and 4, PVDF membrane incubated with ^{125}I-vitronectin. M_r markers: a, β-galactosidase (116000); b, ovalbumin (45000); c, soybean trypsin inhibitor (21500). (**b** and **c**) Binding of ATF to vitronectin. Vitronectin was subjected to limited proteolysis with varying concentrations (mg/ml) of endoproteinase V8 as indicated for 15 min, electrophoresed under reducing conditions on SDS/5–15%-gradient-PAGE gels and transferred to PVDF as described in the Experimental section. (**b**) PVDF membrane stained with Coomassie Blue. (**c**) PVDF membrane incubated with ^{125}I-ATF. M_r markers: 1, myosin (200000); 2, BSA (66000); 3, ovalbumin (45000).

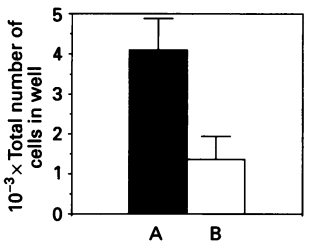

Figure 6 u-PA-mediated U937 adhesion to vitronectin

PMA-stimulated U937 cells were saturated with DFP–u-PA, washed, and incubated on microtitre wells containing immobilized vitronectin as described in the Experimental section. After incubation, plates were washed to remove unattached cells, and adherent cells were removed by trypsin treatment and counted in a haemacytometer. (**a**) Control u-PA-saturated cells; (**b**) u-PA-saturated cells preincubated with soluble vitronectin before addition to vitronectin-coated wells. Error bars signify S.D.

competitively inhibit binding of u-PA to vitronectin was examined by ELISA. Addition of Pg prevents u-PA binding to vitronectin, with approx. 75% inhibition observed at a Pg/u-PA ratio of 0.08:1.0 (Figure 5a). No additional inhibition of binding was observed using Pg concentrations up to a 10-fold excess of u-PA (results not shown). In contrast, PAI-1 does not effectively compete for u-PA binding to vitronectin (Figure 5b), with a maximum of 10% inhibition of binding observed at a PAI-1/u-PA ratio of 5:1.

Role of u-PA–vitronectin interaction in regulation of U937 adhesive activity

Recent evidence suggests that uPAR-associated u-PA promotes adhesion of monocytic U937 cells to vitronectin [26]. In order to assess whether U937 adhesion to vitronectin is mediated via direct u-PA-vitronectin binding as described above, the ability of soluble vitronectin to inhibit competitively binding of u-PA-saturated U937 cells to immobilized vitronectin was determined. Addition of soluble vitronectin at 100 nM inhibited binding of u-PA-saturated U937 cells to immobilized vitronectin by approx. 70% (Figure 6b).

DISCUSSION

Binding of u-PA to uPAR on the surface of many cell types focalizes u-PA activity [19,20]. Pg-binding sites are often co-localized on uPAR-containing cells, facilitating u-PA-catalysed formation of cell-bound plasmin [21–23]. In addition to association with uPAR, interactions of u-PA with several ECM components have recently been reported. For example, Harpel and colleagues described binding of u-PA to the ECM adhesive glycoprotein thrombospondin [17]. Binding was of high affinity (K_d = 40 nM) and did not alter the ability of u-PA to activate Pg. In recent studies, Stephens and colleagues demonstrated that the u-PA kringle domain facilitated interaction of the proteinase with heparin, nidogen and a laminin B1 chain fragment [16,18]. Binding to laminin–nidogen resulted in a 30% decrease in u-PA activity. In addition, an interesting hypothesis was presented suggesting that binding of u-PA to laminin–nidogen may serve primarily as a low-affinity interaction to facilitate loading of uPAR present at cell–matrix junctions [18].

In the present study we have utilized kinetic, ligand blotting and ELISA studies to probe the interaction of u-PA with the ECM proteins collagen type I, collagen type IV, fibronectin, laminin and vitronectin. Initial kinetic studies demonstrated that interaction of u-PA with ECM proteins did not significantly alter the catalytic efficiency ($k_{cat.}/K_m$) of u-PA-catalysed Pg activation. A slight increase (2–4-fold) in $k_{cat.}/K_m$ was observed in the presence of collagen type I, collagen type IV or vitronectin, whereas the presence of laminin and fibronectin resulted in a 3–4-fold decrease in $k_{cat.}/K_m$. Ligand-blotting studies demonstrated that u-PA bound significantly to the ECM-associated adhesive glycoprotein vitronectin. This result was confirmed by ELISA which indicated concentration-dependent, saturable, reversible binding with a $K_{d,app.}$ of 97 nM. Since both ligand-blotting and ELISA studies indicated a specific interaction of u-PA with vitronectin, we performed limited proteolysis of vitronectin followed by ligand-blot analysis with solution-phase u-PA to determine which isolated domain(s) of vitronectin interacted with u-PA. u-PA bound strongly to intact vitronectin as well as two vitronectin-derived fragments of 39 and 49 kDa. Reverse ligand-blot experiments using isolated u-PA domain fragments demonstrated that vitronectin bound to the ATF of u-PA. This result was confirmed in ligand-blotting experiments which demonstrated binding of radiolabelled ATF to intact vitronectin as well as the 39 and 49 kDa fragments. N-terminal sequence analysis indicated that the 49 kDa polypeptide originated with Thr-122 of vitronectin and comprised the hemopexin domain of the molecule, including the heparin-binding region [41].

Vitronectin is an acidic glycoprotein found in association with the ECM of many cell types (for reviews, see [42,41]). The domain structure consists of an N-terminal somatomedin B domain followed by an active RGD-cell attachment sequence. A connecting region joins the somatomedin B domain to two hemopexin-like sequences, the second of which contains a heparin-binding site. Vitronectin has a unique role in regulation of fibrinolysis, resulting from its ability to bind PAI-1. PAI-1 is synthesized in an active form, but readily decays in solution into an inactive, latent form [43,44]. Binding of PAI-1 to vitronectin results in conformational stabilization of PAI-1 such that it retains activity as a functional inhibitor of plasminogen activators [45,46]. These data suggest that binding of PAI-1 to matrix-associated vitronectin may have a role in regulation of pericellular proteolysis [47,11].

Although previous studies have been directed toward identification of binding sites for PAI-1 and Pg on vitronectin, to the best of our knowledge binding of u-PA to vitronectin has not previously been reported. Experiments by Preissner and colleagues demonstrated interaction of Pg with the C-terminal heparin binding domain of vitronectin [11,48]. Additional experiments involving limited proteolysis and synthetic peptides localized a PAI-1-binding site to amino acids 348–370 of the heparin-binding region [48]. Addition of Pg did not interfere with this PAI-1 binding, suggesting that Pg binding was localized to a separate portion of the heparin-binding domain. In contrast, Seiffert and colleagues reported specific binding of PAI-1 to amino acid residues 1–40, which comprise the somatomedin B domain of vitronectin [49,50]. In the present study we report binding of u-PA to a vitronectin-derived polypeptide which comprises the entire hemopexin-like domain of vitronectin, including the heparin binding region. To determine whether the u-PA binding site overlaps with that of Pg or PAI-1, competition ELISAs were performed in which u-PA was bound to vitronectin in the presence of either Pg or PAI-1. Addition of as little as 10 nM Pg (2 pmol) resulted in a significant displacement of u-PA from the vitronectin-coated surface (containing 2.5 pmol of vitronectin). Since the affinity of Pg binding to vitronectin [11] is similar to that of u-PA binding, the ability of low Pg concentrations to effectively block u-PA binding to vitronectin suggests

that the binding sites for Pg and u-PA on vitronectin are the same or overlapping. This is in agreement with Kost et al. [48], who mapped Pg binding to the heparin-binding region of vitronectin. In contrast with Pg, binding of u-PA to vitronectin was not significantly inhibited by up to 500 nM PAI-1 (100 pmol). Although the affinity of PAI-1 for vitronectin is of the same order of magnitude as the u-PA–vitronectin interaction [49], addition of PAI-1 in up to 40-fold excess over the amount of immobilized vitronectin had no effect on binding. This result supports the observations of Seiffert and co-workers [50,51], whose data demonstrated binding of PAI-1 to the N-terminus of vitronectin. Because our experiments utilized DFP-inactivated u-PA, we have identified direct binding of u-PA to vitronectin. However, this does not rule out the possibility that proteolytically active u-PA may also interact with vitronectin-associated PAI-1.

Recent evidence suggests that uPAR-associated u-PA can regulate adhesion of monocytic cells to vitronectin via a mechanism independent of u-PA proteolytic activity [52,25,26]. Binding of U937 cells to vitronectin is mediated via the ATF of uPAR-associated u-PA [26]. To assess whether U937 adhesion to vitronectin is mediated via direct binding of u-PA (or ATF) to vitronectin as described above, the ability of excess u-PA or vitronectin to inhibit competitively binding of u-PA-saturated U937 cells to immobilized vitronectin was determined. Addition of soluble vitronectin resulted in 66% inhibition of uPA-saturated U937 cells to immobilized vitronectin. This is identical with the result reported by Waltz and Chapman [26], who demonstrated a 70% reduction in binding of ^{125}I-vitronectin to u-PA-saturated U937 cells by the addition of excess unlabelled vitronectin. Similarly, preincubation of immobilized vitronectin with u-PA before the addition of u-PA-saturated U937 cells also inhibited binding of U937 cells to immobilized vitronectin. Together these data suggest that the previously observed u-PA-dependent binding of U937 cells to vitronectin is mediated via the direct binding of u-PA to vitronectin as described above, rather than by a u-PA-induced activation of a latent vitronectin receptor on U937 cells, as proposed by Waltz and Chapman [26].

In summary, we have demonstrated a specific, high-affinity, reversible interaction of u-PA with the ECM-associated glycoprotein vitronectin. Binding is mediated via interaction between the ATF of u-PA and the hemopexin domain of vitronectin. u-PA-induced binding of U937 cells to immobilized vitronectin is inhibited by excess free u-PA or vitronectin. Together these data suggest a role for direct binding of u-PA to vitronectin in modulating the adhesiveness of anchorage-independent cells.

We thank Zuzana Valnickova for assistance with N-terminal-sequence analysis. This work was supported by Research Grant CA 58900 (to M.S.S.) from the National Cancer Institute and HL 31932 (to S.V.P.) and HL 49542 (to J.J.E.) from the National Heart, Lung and Blood Institute.

REFERENCES

1 Dano, K., Andreasen, A. P., Grondahl-Hansen, J., Kristensen, P., Nielsen, L. S. and Skriver, L. (1985) Adv. Cancer Res. **44**, 139–266
2 Castellino, F. J. (1981) Chem. Rev. **81**, 431–436
3 Pollanen, J., Saksela, O., Salonen, E. M., Andreasen, P., Nielsen, L., Dano, K. and Vaheri, A. (1987) J. Cell Biol. **104**, 1085–1094
4 Reich, R., Thompson, E. W., Iwamoto, Y., Martin, G. R., Deason, J. R., Fuller, G. C. and Miskin, R. (1988) Cancer Res. **48**, 3307–3312
5 Highsmith, R. F. (1981) J. Biol. Chem. **256**, 6788–6795
6 Ossowski, L. and Vassalli, J. D. (1978) in Biological Markers of Neoplasia: Basic and Applied Aspects (Ruddon, R. W., ed.), Elsevier, Amsterdam
7 Ranby, M. (1982) Biochim. Biophys. Acta **704**, 461–469
8 Nieuwenheuizen, W., Verheijen, J. H., Vermond, A. and Chang, G. T. G. (1983) Biochim. Biophys. Acta **755**, 531–533
9 Knudsen, B. J., Silverstein, R. L., Leung, L. L., Harpel, P. C. and Nachman, R. L. (1986) J. Biol. Chem. **261**, 10765–10771
10 Salonen, E. V., Saksela, O., Vartio, T., Vaheri, A., Neilsen, L. S. and Seuthen, J. (1985) J. Biol. Chem. **260**, 12302–12307
11 Preissner, K. T. (1990) Biochem. Biophys. Res. Commun. **168**, 966–971
12 Stack, M. S., Gonzalez-Gronow, M. and Pizzo, S. V. (1990) Biochemistry **29**, 4966–4970
13 Stack, M. S., Moser, T. L. and Pizzo, S. V. (1992) Biochem. J. **284**, 103–108
14 Moser, T. L., Enghild, J. J., Pizzo, S. V. and Stack, M. S. (1993) J. Biol. Chem. **268**, 18912–18923
15 Stack, M. S. and Pizzo, S. V. (1993) J. Biol. Chem. **268**, 18924–18928
16 Stephens, R. W., Bokman, A. M., Myohanen, H. T., Reisberg, T., Tapiovaara, H., Pedersen, N., Grondahl-Hansen, J., Llinas, M. and Vaheri, A. (1992a) Biochemistry **31**, 7572–7579
17 Harpel, P. C., Silverstein, R. L., Pannell, R., Gurewich, V. and Nachman, R. L. (1990) J. Biol. Chem. **265**, 11289–11294
18 Stephens, R. W., Aumailley, M., Timpl, R., Reisberg, T., Tapiovaara, H., Myohanen, H., Murphy-Ullrich, J. and Vaheri, A. (1992b) J. Biochem. (Tokyo) **207**, 937–942
19 Vassali, J. D., Baccino, D. and Belin, D. (1985) J. Cell Biol. **100**, 86–92
20 Stoppeli, M. P., Corti, A., Soffientini, A., Cassani, G., Blasi, F. and Associan, R. K. (1985) Proc. Natl. Acad. Sci. U.S.A. **82**, 4939–4943
21 Miles, L. A. and Plow, E. F. (1988) Fibrinolysis **2**, 61–71
22 Stephens, R. W., Pollanen, J., Tapiovaara, H., Leung, K. C., Sin, P. S., Salonen, E. M., Ronne, E., Behrendt, N., Dano, K. and Vaheri, A. (1989) J. Cell Biol. **108**, 1987–1995
23 Ellis, V., Behrendt, N. and Dano, K. (1991) J. Biol. Chem. **266**, 12752–12758
24 Ellis, V., Wun, T. C., Behrendt, N., Ronne, E. and Dano, K. (1990) J. Biol. Chem. **265**, 9904–9908
25 Waltz, D. A., Sailor, L. Z. and Chapman, H. A. (1993) J. Clin. Invest. **91**, 1541–1552
26 Waltz, D. A., Chapman, H. A. (1994) J. Biol. Chem. **269**, 14746–14750
27 Novokhatny, V., Medved, L., Mazar, A., Marcotte, P., Henkin, J. and Ingham, K. (1992) J. Biol. Chem. **267**, 3878–3885
28 Cuatracasas, P., Wilcheck, M. and Anfinsen, C. O. (1968) Proc. Natl. Acad. Sci. U.S.A. **61**, 636–643
29 Behrendt, N., Ronne, E., Ploug, M., Petri, T., Loger, D., Nielsen, L. S., Schlenning, W. D., Blasi, F., Appella, E. and Dano, K. (1990) J. Biol. Chem. **265**, 6453–6460
30 Deutsch, D. and Mertz, E. T. (1970) Science **170**, 1095–1096
31 Gonzalez-Gronow, M. and Robbins, K. C. (1984) Biochemistry **23**, 190–196
32 Dahlback, B. and Podack, E. R. (1985) Biochemistry **24**, 2368–2374
33 Wohl, R. C., Summaria, L. and Robbins, K. C. (1980) J. Biol. Chem. **255**, 2005–2013
34 Erlanger, B. F., Kokowsky, N. and Cohen, W. (1965) Arch. Biochem. Biophys. **95**, 271–278
35 Terato, K., Nagai, Y., Kawaniski, K. and Yamomoto, S. (1976) Biochim. Biophys. Acta **445**, 753–762
36 Lineweaver, H. and Burk, D. (1934) J. Am. Chem. Soc. **56**, 658–660
37 Laemmli, U. K. (1970) Nature (London) **227**, 680–685
38 Matsudaria, P. (1987) J. Biol. Chem. **262**, 10035–10038
39 Behrendt, N., Ploug, M., Ronne, E., Hoyer-Hansen, G. and Dano, K. (1993) Methods Enzymol. **223B**, 207–222
40 Suzuki, S., Oldberg, A., Hayman, E. G., Pierschbacher, M. D. and Ruoslahti, E. (1985) EMBO J. **4**, 2519–2524
41 Preissner, K. T. and Jenne, D. (1991) Thromb. Haemostasis **66**, 123–132
42 Tomasini, B. R. and Mosher, D. F. (1990) Prog. Haemostasis Thromb. **10**, 269–305
43 Hekman, C. M. and Loskutoff, D. J. (1985) J. Biol. Chem. **260**, 11581–11587
44 Koistra, T., Sprengers, E. D. and van Hinsbergh, V. W. M. (1986) Biochem. J. **239**, 497–503
45 Mimuro, J. and Loskutoff, D. J. (1989) J. Biol. Chem. **264**, 936–939
46 Seiffert, D. and Loskutoff, D. J. (1991) Biochem. Biophys. Acta **1078**, 23–30
47 Seiffert, D., Wagner, N. N. and Loskutoff, D. J. (1990) J. Cell. Biol. **111**, 1283–1291
48 Kost, C., Stuber, W., Ehrlich, H. J., Pannekoek, H. and Preissner, K. T. (1992) J. Biol. Chem. **267**, 12098–12105
49 Salonen, E., Vaheri, A., Pollanen, J., Stephens, R., Andreasen, P., Mayer, M., Dano, K., Gailit, J. and Ruoslahti, E. (1989) J. Biol. Chem. **264**, 6339–6343
50 Sieffert, D. and Loskutoff, D. J. (1991) J. Biol. Chem. **266**, 2824–2830
51 Seifert, D., Ciambrone, G., Wagner, N. V., Binder, B. R. and Loskutoff, D. J. (1994) J. Biol. Chem. **269**, 2659–2666
52 Nusrat, A. R. and Chapman, H. A. (1991) J. Clin. Invest. **87**, 1091–1097

Received 26 August 1994/23 November 1994; accepted 16 January 1995